Article

Study on the Effect of Two-Stage Injection Strategy for Coal-to-Liquid/Gasoline Reactivity-Controlled Compression Ignition Combustion Mode

Donghui Pan, Wanchen Sun, Liang Guo, Hao Zhang,* Shaodian Lin, and Mengqi Jiang

ACCESS | Metrics & More | Article Recommendations

ABSTRACT: An experimental study was carried out on a modified single-cylinder dual-fuel engine in reactivity-controlled compression ignition (RCCI) mode using pilot fuels with different physicochemical properties, and the effects of the pilot fuels and the two-stage injection strategy on the combustion and emission characteristics of the RCCI mode were explored. The results show that when coal-to-liquid (CTL) is used with a high cetane number as the pilot fuel, the reactivity stratification of the fuel-air mixture is more pronounced. With the advancement of pilot injection timing (SOI1), the heat release rate (HRR) of the CTL/gasoline mode gradually changes from a bimodal pattern to a unimodal pattern. Among them, the bimodal HRR includes CTL premixed combustion and gasoline flame propagation, as well as CTL diffused combustion and gasoline multipoint spontaneous combustion, while the unimodal HRR represents CTL premixed combustion and gasoline multipoint spontaneous combustion. However, the HRR of the fossil diesel/gasoline RCCI combustion mode always exhibits a unimodal form. With the advancement of the main injection timing (SOI2), the gravity center of heat release (CA50) is more advanced when using CTL as the pilot fuel due to the short ignition delay. Overall, compared to fossil diesel, using CTL as the pilot fuel is conducive to controlling the pressure rise rate, which expands the operating range of the RCCI combustion mode. Besides, for both pilot fuels of CTL and fossil diesel, the advancement of SOI1 lowers particle emissions, and the advancement of SOI2 reduces NOx emissions, while the two-stage injection achieves higher indicated thermal efficiency.

Schematic diagram of experimental setup
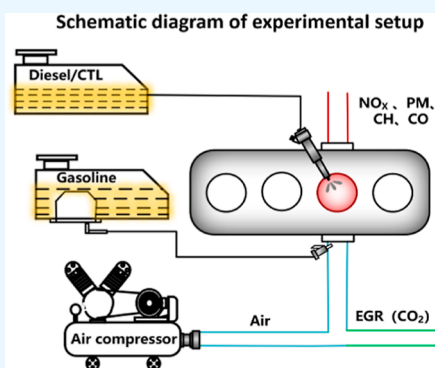
1. INTRODUCTION

Under the background of "carbon peaking and carbon neutrality," the internal combustion engine industry is facing the double challenge of energy and the environment. With the growth of global energy demand and the worsening ecological environment, the coal-to-liquid (CTL) technique, which converts solid coal into liquid fuels in coal-abundant countries, is being developed to adjust and optimize the energy structure, guarantee energy security, and reduce environmental pollution.[1] The characteristics of Chinese energy are "coal-rich, oil-poor, and gas-poor," and coal is very important for the economic and social development of China in the short term.[2] Compared with fossil diesel, CTL from indirect coal liquefaction (DICL) has a high cetane number (CN), lower aromatics, and a lower boiling range. The combustion of CTL is more stable and produces lower PM, CO, and HC emissions,[3] so it is a high-quality diesel alternative fuel.[4] Besides, CTL as the base fuel can be intermixed with fossil diesel fuels in any ratio and has broad application prospects in internal combustion engines.[5,6]

To achieve high efficiency and clean combustion in compression ignition (CI) engines, scholars have conducted many new combustion technologies, including homogeneous charge compression ignition,[7] premixed charge compression ignition (PCCI),[8] and reactivity-controlled compression ignition (RCCI).[9] Cheng et al.[10] studied the realization of the PPC combustion mode in a heavy-duty diesel engine with a single injection strategy, and the results showed that both early and late fuel injection strategies contributed to a more homogeneous mixture and made the diffusion combustion phase disappear. Klingbeil et al.[11] found that early or late injection with large exhaust gas recirculation (EGR) rates resulted in ultralow emissions for heavy-duty diesel engines under low speeds and under low loads, while the early injection strategy resulted in better emission results at high speeds and low loads. Besides, the RCCI mode, which can improve engine thermal efficiency and reduce ultralow NOx and PM emissions, is therefore receiving a lot of attention. RCCI combustion mode generally injects the low-reactivity (low CN) fuel into

(a) CTL/gasoline RCCI combustion mode   (b) Fossil diesel/gasoline RCCI combustion mode
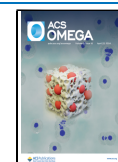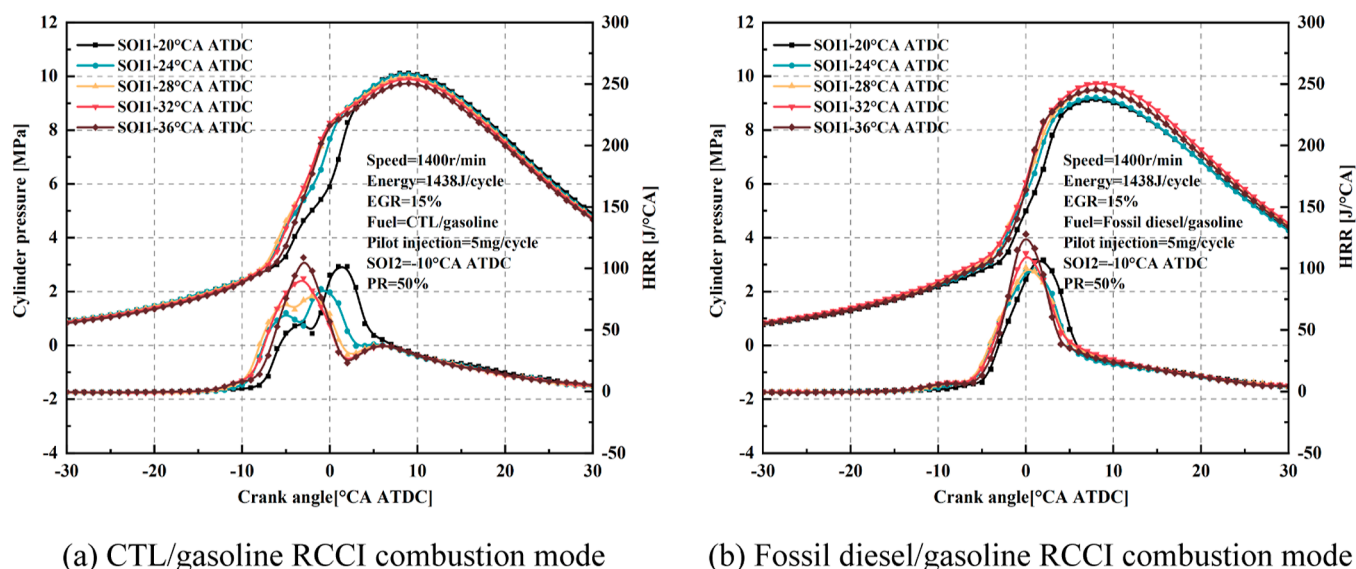
Figure 1. Effects of SOI1 on cylinder pressures and HRRs of CTL/gasoline and fossil diesel/gasoline RCCI combustion modes.

the engine intake and directly injects the fuels with high-reactivity (high CN) into the cylinder. These two fuels form a homogeneous fuel-air mixture in the cylinder, which can control the combustion phasing and slow down the pressure rise rate (PRR) and the heat release rate (HRR).[12] Liu et al.[13−16] carried out some experiments on the combustion characteristics of RCCI combustion mode using different characteristics of fuels combined with an injection strategy. The results show that they have a great influence on the combustion characteristics of RCCI, fuel proportion, equivalence ratio, injection sequence, or injection timing.

Because of the high CN of CTL, it can be used for PCCI and RCCI combustion modes. In our research group, PCCI and RCCI combustion modes were studied in a CI engine using CTL as the base fuel. Sun et al.[17] blended CTL with gasoline to form a wide distillation fuel and injected it into the cylinder. The combustion and emission characteristics of the PCCI combustion mode were studied under various starts of injection (SOI) along with the addition of EGR. Experimental results showed that the blending of CTL/gasoline resulted in a higher premixed combustion ratio (PCR) and reduced NOx and particulate emissions. Zhang et al.[18,19] conducted experimental studies on the combustion and emission characteristics of CTL/gasoline and CTL/*n*-butanol dual-fuel modes. The results showed that the RCCI using CTL as the ignition fuel had a shorter combustion duration (CD), a 2% increase in the indicated thermal efficiency (ITE), and the peak pressure rise rate (PPRR) and NOx emissions were reduced by 46.1 and 20.1%, respectively. The CTL/*n*-butanol dual fuel mode with a 30% *n*-butanol ratio showed a 49.5% reduction in NOx emission and a 40.9% reduction in particulate matter emission compared with the pure CTL mode. Sun et al.[20] carried out an experiment on engine combustion and emission characteristics of CTL/gasoline and diesel/gasoline RCCI combustion mode under low load. The results showed that both CTL/gasoline and diesel/gasoline RCCI combustion modes contain distinguishable low-temperature and high-temperature heat release, and CA50 of the CTL/gasoline RCCI combustion mode was more advanced. In addition, the CTL/gasoline RCCI combustion mode reduced the emissions of CO, HC, and particles under optimum intake conditions.

The RCCI combustion mode with the two-stage injection strategy can further reduce engine emissions and meet ultralow emission regulations. Under the two-stage injection strategy, the adoption of SOI1, SOI2, mass injection ratio, injection duration, and fuel characteristics can achieve combustion control and reduce pollutant emissions.[21−24] Many researchers used the pilot injection strategy in the RCCI combustion mode and investigated the combustion and emission characteristics of dual-fuel engines under different operating conditions.[25−32] Those results showed that the use of the pilot injection strategy could significantly change the in-cylinder combustion process in dual-fuel engines and reduce the emissions of pollutants such as total hydrocarbons (THC), CO, and so forth, but NOx emissions increase slightly. Lu[33] and Wang et al.[34] studied the effect of SOI1 on the combustion and emission characteristics of RCCI mode under high-load and low-speed conditions. The results showed that earlier SOI1 and increasing pilot injection fuel mass ratio could reduce NOx emissions. The pilot injection strategy with EGR[35−38] can reduce HC, CO, and NOx emissions of the dual-fuel engine. Liu et al.[39] studied the effects of SOI1 and pilot injection mass ratio on the combustion performance and emissions in natural gas/diesel dual-fuel RCCI combustion mode. The results showed that when the SOI1 was varied from −15 to 27 crank angle after TDC, the IMEP and PRR were increased, while the CO, HC, soot, and CH4 emissions were reduced. The literature review presented above shows that the fuel characteristics and injection strategies significantly affect the combustion and emission characteristics of the RCCI combustion mode. Previous studies of our research group have shown that CTL with high CN as the ignition fuel of RCCI combustion mode is conducive to improving the thermal efficiency of the engine.[17−20] However, the use of CTL as a pilot fuel with a two-stage injection strategy in dual-fuel engines is expected to further improve the thermal efficiency of the engine, thus expanding the operating range of the RCCI combustion mode. But related research has been reported. For the RCCI mode that adopts CTL as the pilot fuel, it is necessary to explore the effects of the two-stage injection strategy on combustion and emission characteristics.
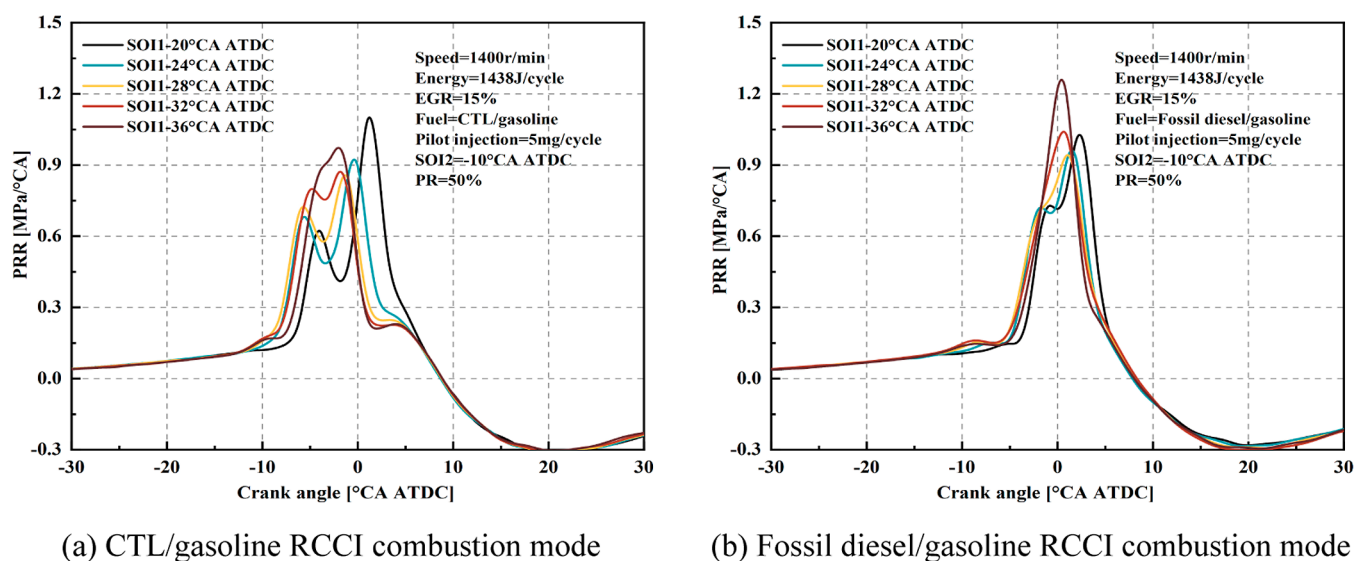
(a) CTL/gasoline RCCI combustion mode

(b) Fossil diesel/gasoline RCCI combustion mode

Figure 2. Effects of SOI1 on PRR of CTL/gasoline and fossil diesel/gasoline RCCI combustion modes.

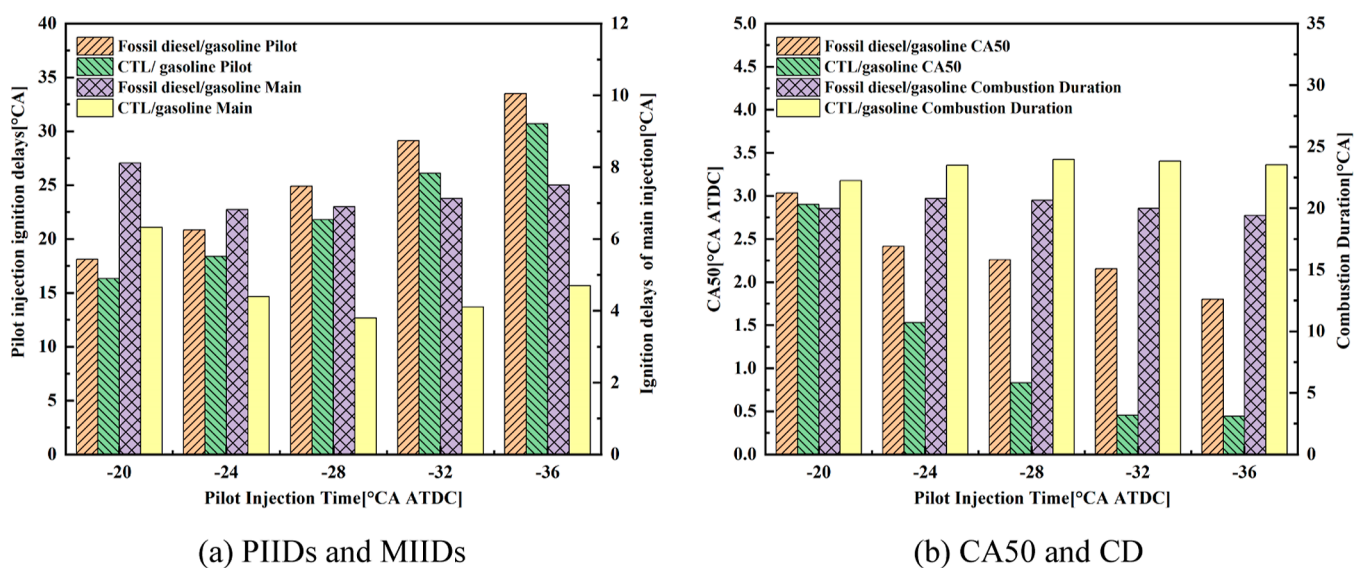(a) PIIDs and MIIDs

(b) CA50 and CD

Figure 3. Effects of SOI1 on IDs, CA50s, and CDs of CTL/gasoline and fossil diesel/gasoline RCCI combustion modes.

In this study, an experiment on a CI engine with a two-stage injection strategy was carried out to investigate the effects of SOI1, SOI2, and fuel characteristics on the combustion and emission characteristics of CTL/gasoline and fossil diesel/gasoline under the RCCI combustion mode. The injection strategy for the RCCI mode that adopts CTL as the pilot fuel was explored.

2. RESULTS AND DISCUSSION

2.1. Effects of SOI1 and Fuel Characteristics on RCCI Combustion Characteristics. Figure 1 shows the effects of SOI1 on the cylinder pressures and HRRs of CTL/gasoline and fossil diesel/gasoline RCCI combustion modes. As seen in Figure 1, the cylinder pressure of the CTL/gasoline RCCI combustion mode gradually decreases with the advancement of SOI1, while the peak cylinder pressure of the fossil diesel/gasoline RCCI combustion mode increases at first and then decreases. With the advancement of SOI1, the mixing time for fuel and air increases, and the equivalent ratio of the premixed fuel is reduced, so the combustion rate becomes slow and

results in a gradual decrease with the cylinder pressure peak of the CTL/gasoline RCCI combustion mode. Besides, with the advancement of SOI1, the HRR of CTL/gasoline RCCI combustion mode exhibits a bimodal pattern, and the value of the second peak increases at first and then decreases whereas the HRR of fossil diesel/gasoline RCCI combustion mode exhibits a unimodal pattern with a higher peak. In particular, due to the high CN of CTL, as SOI1 advances from −20 to −28 °CA ATDC, the first peak of the HRR is formed by the premixed combustion of CTL and the flame propagation of gasoline at the early stage of ignition, and the second peak of the HRR is formed by the diffusion combustion of CTL and the multipoint spontaneous combustion of gasoline. AS SOI1 varies from −32 to −36 °CA ATDC, mixtures of pilot CTL, gasoline, and air are more homogeneous, and gasoline combustion is transformed from flame propagation to multipoint autoignition; thus, the accelerated combustion rate makes the HRR of the CTL/gasoline RCCI gradually change from a bimodal shape to a unimodal shape. Compared to the CTL, the fossil diesel with a lower CN as a pilot fuel of

the RCCI combustion mode has a longer ignition delay (ID) and a higher PCR, which leads to a unimodal shape with a higher peak of the HRR. From Figure 2, furthermore, the PPRR of the CTL/gasoline RCCI combustion mode is lower than that of the fossil diesel/gasoline RCCI combustion mode. Therefore, the use of CTL as a pilot injection fuel is conducive to the expansion of the operation load range of RCCI combustion mode.

Figure 3 shows the effects of SOI1 on the combustion characteristics of CTL/gasoline and fossil diesel/gasoline RCCI combustion modes. From Figure 3a, it can be seen that the pilot injection ignition delays (PIIDs) of CTL/gasoline and fossil diesel/gasoline RCCI combustion modes increase with the advancement of the SOI1, and the ID of the CTL/gasoline RCCI combustion mode is relatively short. As SOI1 varies from −20 °CA ATDC to −36 °CA ATDC, the PIID is prolonged. Since the CTL has higher CN than fossil diesel, it reaches the ignition condition earlier than fossil diesel, and it has a shorter ID. Besides, as shown in Figure 3b, compared with the fossil diesel/gasoline RCCI combustion mode, the CTL/gasoline RCCI combustion mode has a more advanced CA50 and a longer CD. Since the CTL has higher CN than fossil diesel, the ID is shorter when the CTL is used as the pilot fuel in the RCCI combustion mode. The diffusion combustion proportion of CTL is increased, which leads to the prolongation of CD in the CTL/gasoline RCCI combustion mode.

Figure 4 shows the effects of SOI1 on fuel consumption rates and ITEs of CTL/gasoline and fossil diesel/gasoline
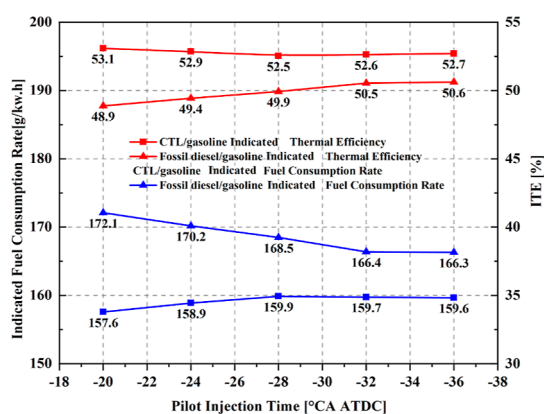

Figure 4. Effects of SOI1 on the fuel economy of CTL/gasoline and fossil diesel/gasoline RCCI combustion modes.

RCCI combustion modes. As shown in Figure 4, with the advancement of SOI1, the ITE of the fossil diesel/gasoline RCCI combustion mode gradually and finally becomes flat, and the fuel consumption rate decreases. Whereas the ITE of the CTL/gasoline RCCI combustion mode is slightly affected by the SOI1 and is higher than that of the fossil diesel/gasoline RCCI combustion mode. This is due to when using CTL as the pilot fuel of the RCCI combustion mode, the ID is shorter, the CA50 is forward, and CD is longer than the pilot fuel of fossil diesel. Besides, the combustion temperature is lower, resulting in lower heat transfer losses, and therefore, the CTL/gasoline of the RCCI combustion mode has a better fuel economy than fossil diesel/gasoline RCCI combustion mode.

2.2. Effects of SOI2 and Fuel Properties on RCCI Combustion Characteristics. Figures 5 and 6 show the

effects of SOI2 on cylinder pressures, HRRs, and PRRs of CTL/gasoline and fossil diesel/gasoline RCCI combustion modes. As shown in Figure 5, the peak cylinder pressures of the CTL/gasoline and fossil diesel/gasoline RCCI combustion modes increase as SOI2 is advanced. The main reason is that when the pilot fuel CTL and fossil diesel are injected into the cylinder, the fire starts to burn immediately, and the peak cylinder pressure rises. It can also be seen from the figure that the HRRs of both CTL/gasoline and fossil diesel/gasoline RCCI combustion modes exhibit the bimodal shapes that include the self-ignite of gasoline and ignition fuel as well as the diffusion combustion of ignition fuel. When the main injection fuel is injected into the cylinder (−10 °CA ATDC), the pilot fuel has already begun to burn, the main injection fuel is mainly involved in the diffusion combustion, therefore the HRR exhibits a bimodal. Since the fossil diesel has a lower CN than the CTL, the fossil diesel/gasoline RCCI combustion mode has a long ID (as shown in Figure 8b), so that more sufficient mixing of the fuel and air formed before ignition, and the premixed combustion heat release is faster, so the PPRR of the fossil diesel/gasoline RCCI combustion mode is higher than that of the CTL/gasoline RCCI combustion mode. From Figure 6, it can be seen that the PPRRs for both CTL/gasoline and fossil diesel/gasoline RCCI combustion modes are the maximum when SOI2 is −12 °CA ATDC, and the maximum PPRR of the CTL/gasoline RCCI combustion mode is generally lower than that of the fossil diesel/gasoline RCCI combustion mode, so CTL is beneficial to the expansion of the operation load range for the RCCI combustion mode.

Figure 7 shows the effects of SOI2 on the combustion characteristics of the CTL/gasoline and fossil diesel/gasoline RCCI combustion modes. As can be seen from Figure 8a, the main injection ignition delays (MIIDs) of both CTL/gasoline and fossil diesel/gasoline RCCI combustion modes increase with the advancement of SOI2, and the MIIDs of CTL/gasoline RCCI combustion mode are shorter than those of fossil diesel/gasoline RCCI combustion mode. The main reason is that the pilot injection fuel first ignites the mixture of gasoline and air, and the main injection fuel is injected into the cylinder immediately and begins to burn. Moreover, CTL is more reactive than fossil diesel fuel so MIID is shorter. As shown in Figure 8b, due to the short ID of CTL and the overall advancement of the combustion phase, the CA50 of the CTL/gasoline RCCI combustion mode is more forward than that of the fossil diesel/gasoline RCCI combustion mode, and the CD is prolonged due to the slow diffusion combustion rate of CTL in the later stage.

Figure 8 shows the effects of SOI2 on the fuel economy of CTL/gasoline and fossil diesel/gasoline RCCI combustion modes. As shown in Figure 8, the ITE of CTL/gasoline and fossil diesel/gasoline RCCI combustion modes gradually increase with the advancement of SOI2, and the ITE of the CTL/gasoline RCCI combustion mode is higher than that of the fossil diesel/gasoline RCCI combustion mode. The fuel consumption rate of CTL/gasoline and fossil diesel/gasoline RCCI combustion mode decreases gradually with the advancement of SOI2, but the fuel consumption rate of CTL/gasoline is lower than fossil diesel/gasoline. The main reason is that CTL as the pilot fuel has a short ID, an advanced CA50, and a long CD, so it indicates a high ITE. When SOI2 is −12 °CA ATDC, the ITE of the CTL as the main injection fuel increases to 3.5% compared with the fossil diesel as the pilot fuel. When using the CTL as the pilot fuel, the fuel consumption rate is
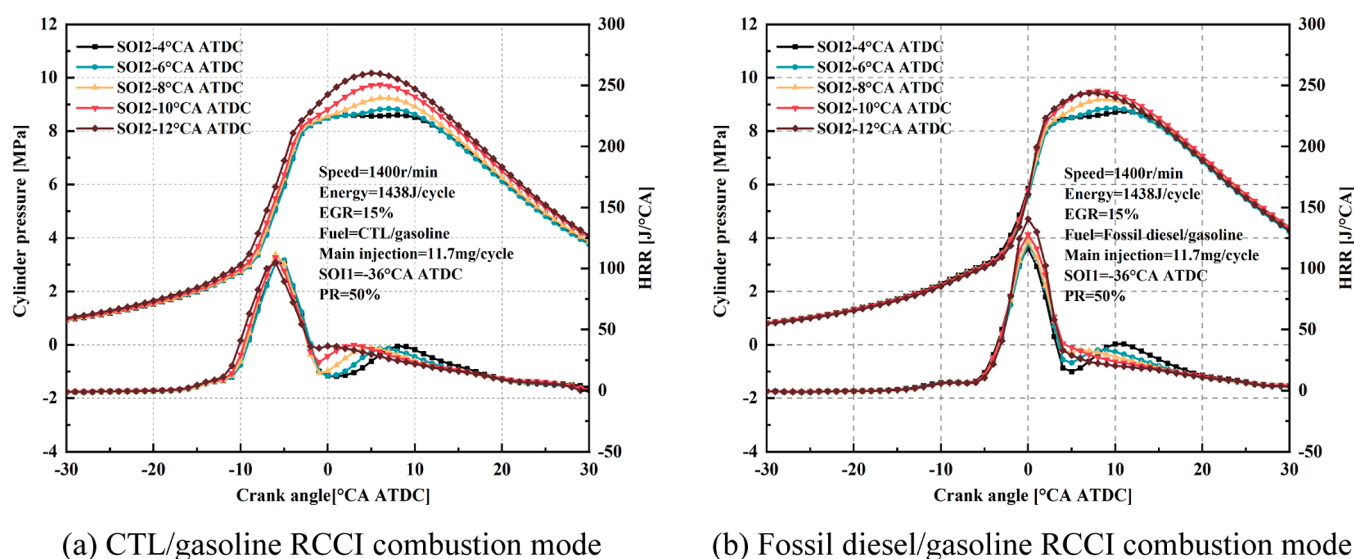
(a) CTL/gasoline RCCI combustion mode

(b) Fossil diesel/gasoline RCCI combustion mode

Figure 5. Effects of SOI2 on cylinder pressures and HRRs of CTL/gasoline RCCI and fossil diesel/gasoline RCCI combustion modes.

(a) CTL/gasoline RCCI combustion mode
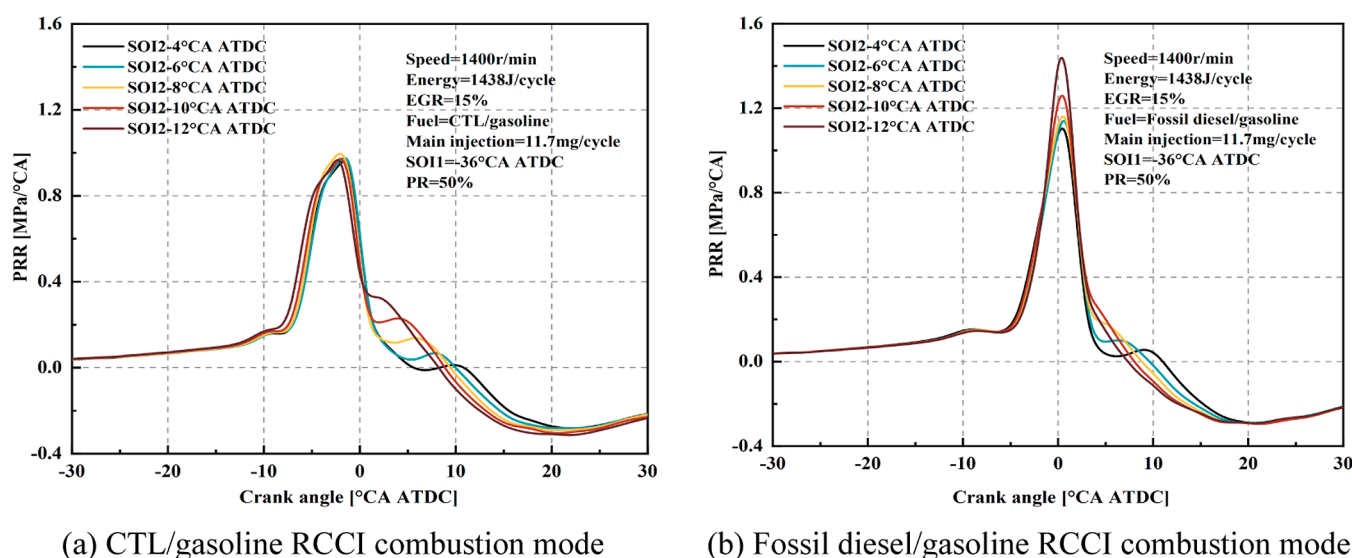
(b) Fossil diesel/gasoline RCCI combustion mode

Figure 6. Effects of SOI2 on PRRs of CTL/gasoline and fossil diesel/gasoline RCCI combustion modes.

156.3 g/kw h, which is reduced by 15.6 g/kw h, relative to the fossil diesel as the pilot fuel.

2.3. Effects of Two-Stage Injection Strategy and Fuel Characteristics on Emission Characteristics in the RCCI Combustion Mode. Figure 9 shows the effects of SOI1 on pollutant emissions in CTL/gasoline and fossil diesel/gasoline RCCI combustion modes. As shown in Figure 9a, the NOx emissions of both the CTL/gasoline and fossil diesel/gasoline RCCI combustion modes first increase and then decrease with the advanced SOI1, while soot emission is the opposite. From Figure 10a, the more even mixture of fuel and air with SOI1 varying from −20 °CA ATDC to −28 °CA and the higher PHRR lead to a higher peak of combustion temperature and lasts for a long time, which promotes the generation of NOx; however, it is conducive to inhibiting the generation of soot. The mixture equivalent ratio is more uniform with SOI1 varying from −32 °CA ATDC to −36 °CA, and the lower PHRR leads to a lower peak of combustion temperature, which suppresses the generation of NOx. Besides, the late oxidation of soot is weakened with SOI1 varying from −32 °CA ATDC

to −36 °CA, therefore soot emissions are higher. The overall trend shows that the CTL/gasoline RCCI combustion mode has higher NOx emissions than the fossil diesel/gasoline RCCI combustion model, while the soot emissions are lower than the fossil diesel/gasoline RCCI combustion mode. When using the CTL/gasoline mode with the two-stage injection results in a more even mixture of fuel and air, a longer CD, a higher peak of combustion temperature, and a longer high-temperature duration than the fossil diesel/gasoline mode, so the NOx emissions of the CTL/gasoline RCCI combustion mode are higher than the fossil diesel/gasoline RCCI combustion mode. As shown in Figure 9b, the HC emissions of both CTL/ gasoline and fossil diesel/gasoline RCCI combustion modes increase at first and then decrease with the advanced SOI1. When SOI1 is advanced from −20 °CA ATDC to −24 °CA ATDC, the HC emission of the CTL/gasoline RCCI combustion mode is lower than that of the fossil diesel/ gasoline RCCI combustion mode. When SOI1 is advanced from −28 °CA ATDC to −36 °CA ATDC, the HC emission of the CTL/gasoline RCCI combustion mode is slightly higher
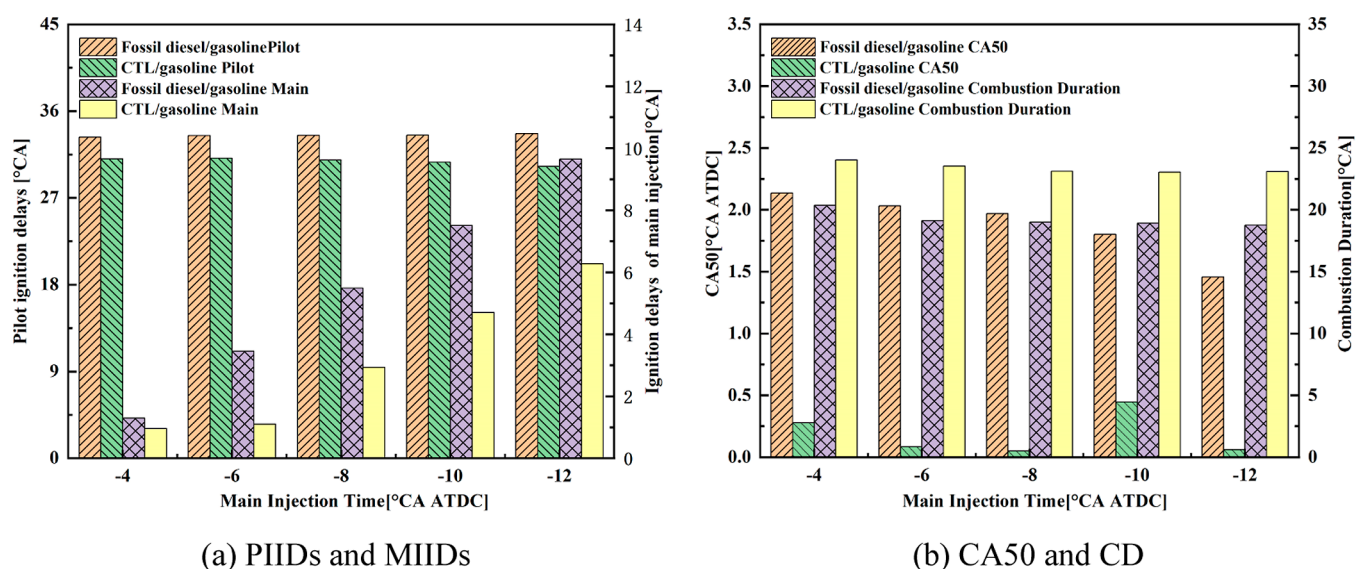
(a) PIIDs and MIIDs

(b) CA50 and CD

Figure 7. Effects of SOI2 on the IDs, CA50s, and CDs of CTL/gasoline and fossil diesel/gasoline RCCI combustion modes.
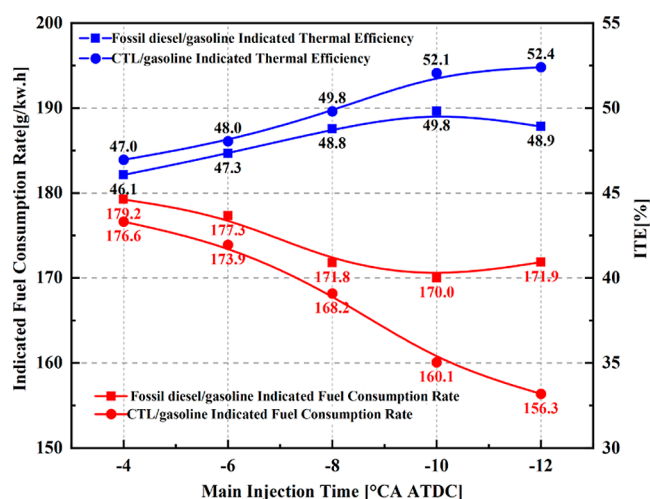

Figure 8. Effects of SOI2 on the fuel economy of CTL/gasoline and fossil diesel/gasoline RCCI combustion modes.

than the fossil diesel/gasoline RCCI combustion mode. The reason is that during the combustion process, some fuel adheres to the cylinder wall, resulting in increased HC emissions. Since the CTL has greater reactivity and a higher temperature, it is beneficial to reduce HC emissions. Moreover, the CO emissions of CTL/gasoline and fossil diesel/gasoline RCCI combustion modes decrease first and then increase with the advancement of the SOI1. From Figure 10b, when SOI1 is between −20 °CA ATDC to −24 °CA ATDC, the evaporation time and the mixing time of the fuel and air are more sufficient in the cylinder, and the combustion efficiency of CTL/gasoline RCCI combustion mode is higher than that of the fossil diesel/gasoline, so the CO emissions of CTL/gasoline and fossil diesel/gasoline RCCI combustion modes are reduced. When the earlier SOI1 is between −28 °CA ATDC and −36 °CA ATDC, the mixture is easy to produce the stratification of temperature and concentration during the premixed combustion, forming local low temperature and fuel-lean zones, increasing the degree of incomplete
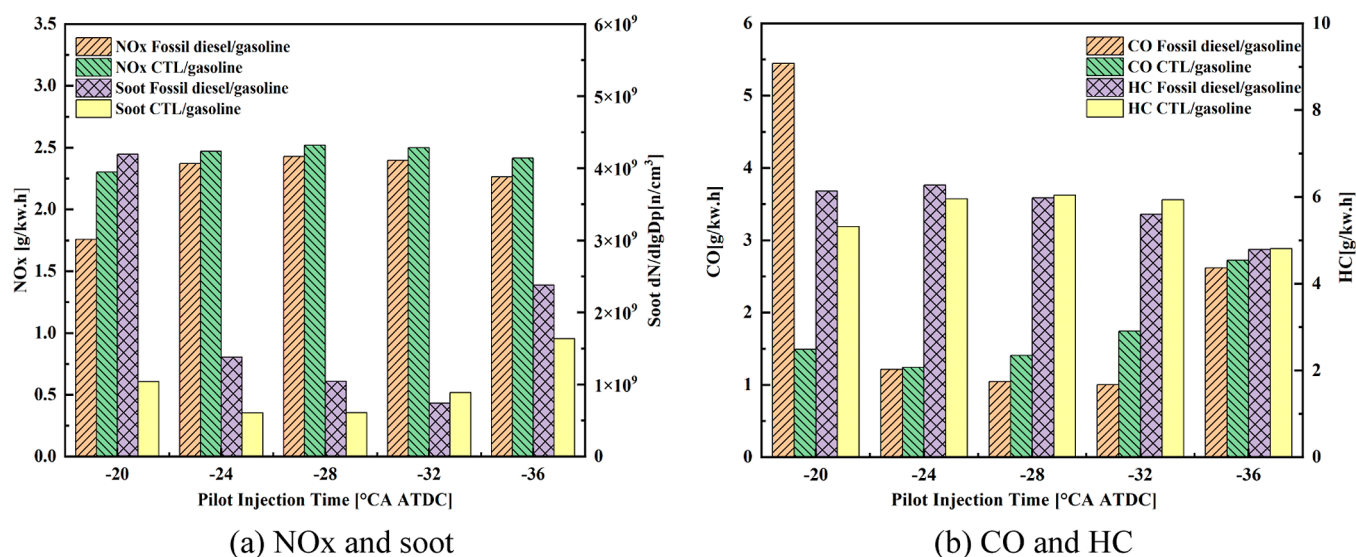

(a) NOx and soot

(b) CO and HC

Figure 9. Effects of SOI1 on CTL/gasoline and fossil diesel/gasoline RCCI combustion modes on pollutant emissions.

（a）The peak of combustion temperature
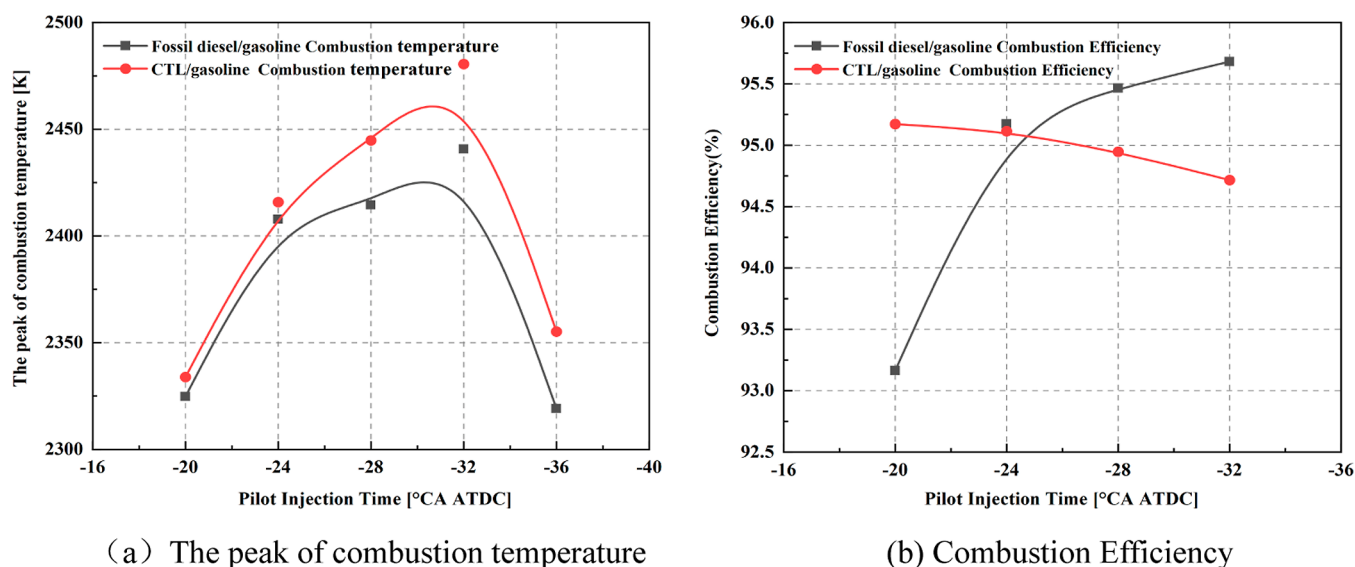
(b) Combustion Efficiency

Figure 10. Effects of SOI1 on the CTL/gasoline and fossil diesel/gasoline RCCI combustion modes on the peak of combustion temperature and combustion efficiency.
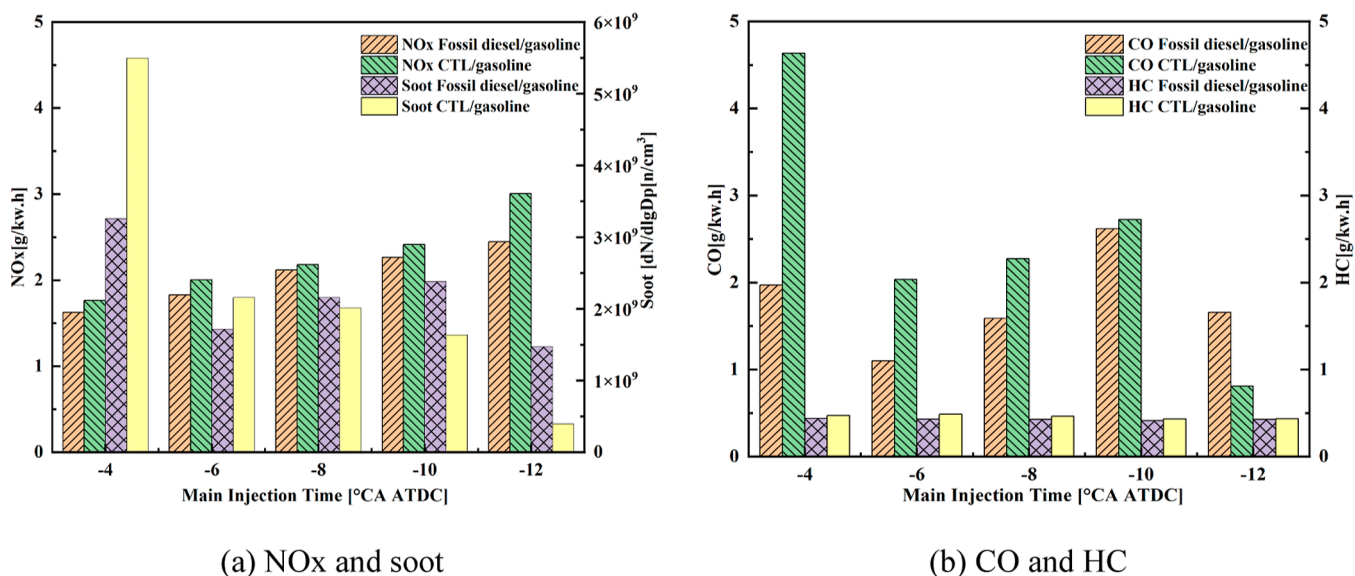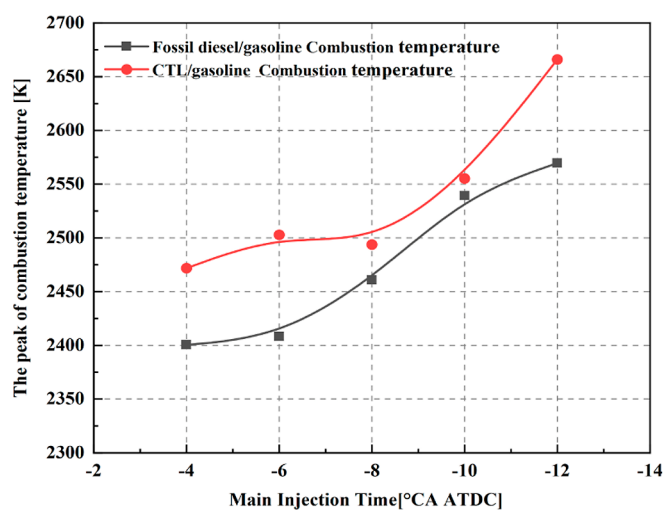

(a) NOx and soot

(b) CO and HC

Figure 11. Effects of SOI2 on CTL/gasoline and fossil diesel/gasoline RCCI combustion modes on pollutant emissions.

combustion and the higher CO emissions. The combustion efficiency of CTL/gasoline is lower than that of the fossil diesel/gasoline; therefore, the CO emission of the CTL/gasoline RCCI combustion mode is higher than that of the fossil diesel/gasoline RCCI combustion mode.

Figure 11 shows the effects of SOI2 on pollutant emissions from the CTL/gasoline and fossil diesel/gasoline RCCI combustion modes. Figure 11a shows that as the SOI2 is advanced, the NOx emissions of both CTL/gasoline and fossil diesel/gasoline RCCI combustion modes increase, and the NOx emissions of CTL/gasoline in RCCI combustion mode are higher than those of fossil diesel/gasoline RCCI combustion mode. In contrast, the soot emissions of both CTL/gasoline and fossil diesel/gasoline RCCI combustion modes decrease. Compared with the fossil diesel/gasoline RCCI combustion mode, the soot emissions of CTL/gasoline in RCCI combustion mode are higher. Because of the CTL with high activity, as SOI2 advanced, the concentration

stratification of a mixture of fuel and air can be effectively improved. Figure 12a shows that the CTL/gasoline RCCI combustion mode with a higher peak of combustion temperature than the diesel/gasoline RCCI combustion mode leads to an increase in NOx emissions and a decrease in the soot emissions of the CTL/gasoline RCCI combustion mode.

From Figure 11b, it can be seen that the HC emissions of both CTL/gasoline and fossil diesel/gasoline RCCI combustion modes are essentially unchanged with the SOI2 advanced. When the SOI2 varies from −6 °CA ATDC to −10 °CA ATDC, the CO emissions of both CTL/gasoline and fossil diesel/gasoline RCCI combustion modes increase, and the CO emissions of CTL/gasoline combustion mode are higher than those of fossil diesel/gasoline RCCI combustion mode. Due to the CTL with high CN and uneven mixing of fuel and air, this leads to low combustion efficiency (Figure 12b) and a larger amount of CO emissions produced. When SOI2 is before −6

（a）The peak of combustion temperature
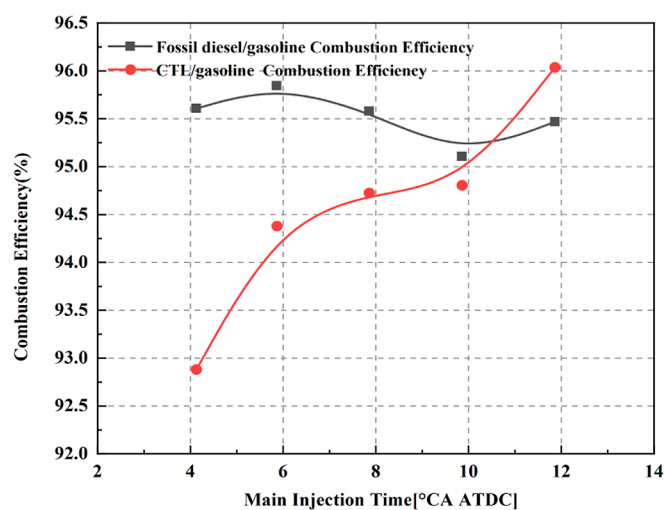
（b）Combustion Efficiency

Figure 12. Effects of SOI2 on CTL/gasoline and fossil diesel/gasoline RCCI combustion modes on the peak of combustion temperature and combustion efficiency.

°CA ATDC, the CO emissions of both CTL/gasoline and fossil diesel/gasoline RCCI combustion modes are lower, and the CTL as a pilot fuel is higher as SOI2 advanced than fossil diesel. This is due to the advancement of SOI2, the moving uniformity of the mixture of fuel and air, and the higher temperature, which leads to combusting enough and reducing CO emissions. Since the CTL is a pilot fuel with a longer CD, the CO emissions of the CTL/gasoline RCCI combustion mode are higher than those of fossil diesel/gasoline RCCI combustion mode.

3. CONCLUSIONS

This study carried out experimental research on the RCCI mode with different physicochemical properties of the pilot fuel to investigate the effects of fuel characteristics and a two-stage injection strategy on the combustion and emission characteristics of the RCCI combustion mode. The injection strategy of the RCCI combustion mode suitable for CTL, which is used as the pilot fuel with high reactivity, is proposed. The conclusions can be summarized as follows:

1 In the RCCI combustion mode with two-stage injection, with SOI1 advancing from −20 to −28 °CA ATDC, the HRR of CTL/gasoline RCCI combustion mode is a bimodal pattern. With SOI1 advancing from −32 to −36 °CA ATDC, gasoline combustion changes from flame propagation to multipoint spontaneous combustion, so that the CTL/gasoline RCCI combustion mode changes from a bimodal pattern to a unimodal pattern. The PPRR of CTL/gasoline RCCI combustion mode is lower than fossil diesel/gasoline RCCI combustion mode, and the use of high-reactivity CTL as the pilot fuel is conducive to reducing the PPRR and expanding the operating load range of RCCI combustion mode.

2 Under the two-stage injection strategy of RCCI combustion mode, the fuel economy of CTL as the pilot fuel is better than fossil diesel. The ITE of the fossil diesel/gasoline RCCI combustion mode increases with the advancement of SOI1, while the ITE of CTL/gasoline is slightly affected by SOI, and the fuel consumption rates of both CTL/gasoline and fossil

diesel/gasoline RCCI combustion modes decrease with the advancement of SOI1. With the advancement of SOI2, the ITE of both CTL/gasoline and fossil diesel/gasoline RCCI combustion modes increase, and the fuel consumption rate of those decreases. In general, compared to the fossil diesel/gasoline RCCI combustion mode, the CTL/gasoline RCCI combustion mode shows higher ITE and lower fuel consumption rates.

3 Under the two-stage injection strategy of RCCI combustion mode, compared to the fossil diesel, the CTL with high reactivity as the pilot fuel is conducive to reducing particulate emissions. With the advancement of SOI1, the mixture of fuel and air is locally excessively fuel-lean and difficult to produce soot for both CTL/gasoline and diesel/gasoline RCCI combustion modes, and particulate emissions of CTL/gasoline RCCI combustion mode are slightly higher. When SOI1 and SOI2 are advanced, the NOx emissions of CTL/gasoline RCCI combustion mode are higher than diesel/gasoline RCCI combustion mode, while lower soot emissions can be obtained for CTL/gasoline RCCI combustion mode than diesel/gasoline RCCI combustion mode. The advancement of SOI1 results in less amount of fuel attached to the wall, therefore HC emissions are significantly decreased.

4. EXPERIMENTAL SYSTEM AND TEST PROCEDURE

4.1. Experimental Engine and Apparatus. The test engine was converted from a high-pressure common rail four-cylinder diesel engine to a single-cylinder engine, and only the third cylinder had independent intake, exhaust, and fuel injection systems. The intake and exhaust manifolds of the other three cylinders, as well as the injectors, were removed from the original engine. The third cylinder was equipped with a simulated supercharging system and an EGR system and then controlled the EGR rate by adjusting the EGR valve. The air intake system was provided by the compressor as the air source, and the outlet of the compressor was equipped with primary and secondary stabilizer tanks to regulate the intake pressure of the test engine between 0 and 0.35 MPa (gauge
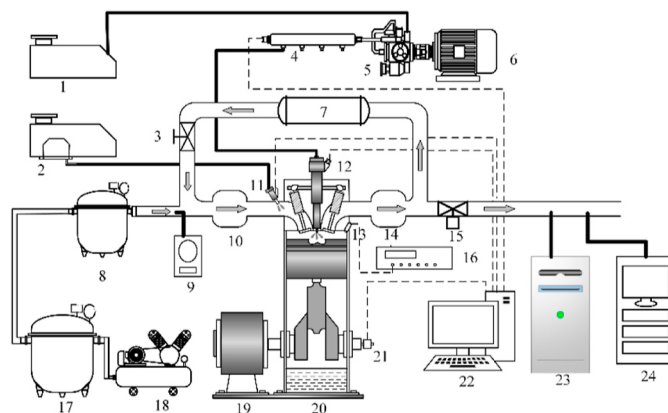
1: CTL/diesel tank; 2: Gasoline tank; 3: EGR valve; 4: High pressure oil rail; 5: High pressure oil pump; 6: Alternating current motor; 7: EGR intercooler; 8: Second-stage surge tank; 9: Air flow meter; 10: Intake pressure surge tank; 11: PFI injector; 12: DI injector; 13: Cylinder pressure sensor;14: Exhaust pressure surge tank; 15: Exhaust back-pressure valve; 16: Combustion analyzer; 17:First-stage surge tank; 18: Air compressor; 19: Dynamometer; 20: Engine; 21: Photoelectric encoder;22: Computer; 23: Emission analyzer; 24 : Particle Analyzer;

Figure 13. Schematic diagram of the experimental setup. (1) CTL/diesel tank; (2) gasoline tank; (3) EGR valve; (4) high-pressure oil rail; (5) high-pressure oil pump; (6) alternating current motor; (7) EGR intercooler; (8) second-stage surge tank; (9) air flow meter; (10) intake pressure surge tank; (11) PFI injector; (12) DI injector; (13) cylinder pressure sensor; (14) exhaust pressure surge tank; (15) exhaust back-pressure valve; (16) combustion analyzer; (17) first-stage surge tank; (18) air compressor; (19) dynamometer; (20) engine; (21) photoelectric encoder; (22) computer; (23) emission analyzer; and (24) particle analyzer.

pressure) through a limiting valve. The fuel injection system included an intake port injection system and an in-cylinder direct injection system. In addition, the temperature of the engine cooling water was maintained at 353 ± 1 K. The schematic diagram of the experimental setup is shown in Figure 13, and the engine specification is shown in Table 1.

Table 1. Engine Specification

category	properties
geometric compression ratio	17.1
cylinder diameter/mm	95.4
piston stroke/mm	104.9
connecting rod length/mm	162
DI injector orifice number	7
eddy current ratio	0.97

4.2. Methodology and Test Conditions. In this study, the engine speed was fixed at 1400 rpm, the per-cycle energy was 1438J/cycle for all test fuels, and the injection pressure was 100 MPa. The effects of the two-stage injection strategies of CTL and fossil diesel on the performance, combustion, and emission characteristics were investigated in the RCCI combustion mode. In this study, gasoline was injected through the intake port, and its proportion in the cycle energy was fixed at 50%, while CTL and fossil diesel were injected into the cylinder by the "pilot injection + main injection". To control the combustion process and prevent the engine from working roughly, 15% EGR was introduced into the intake. This experimental study utilizes two-stage injection strategies in order to better understand the effect of main and pilot timing on combustion. The PIID and the MIID are defined separately, and CA10 is the crankshaft angle at the combustion start point. The equations are as follows: eqs 1 and 2.

$$PIID = SOI1 - CA10 \tag{1}$$

$$MIID = SOI2 - CA10 \tag{2}$$

The other equations are as follows: eqs 3−7.

$$W_i = \int P dV \tag{3}$$

where W_i represents the indication of the function. P represents the cylinder pressure. V represents the cylinder pressure and the combustion chamber volume.

$$\eta_i = \frac{W_i}{g_{gasoline} H_{u,gasoline} + g_{fuel} H_{u,fuel}} \tag{4}$$

where η_i represents indicative thermal efficiency. $g_{gasoline}$ represents the fuel consumption of gasoline. g_{fuel} represents the fuel consumption of the fuel. $H_{u,gasoline}$ represents the low calorific value of gasoline. $H_{u,fuel}$ is the low calorific value of fuel.

$$b_i = \frac{B}{P_i} = \frac{120 i \cdot n \cdot g_b}{\tau} \Big/ \frac{W_i}{t} \tag{5}$$

where b_i represents indicated specific fuel consumption. i represents the number of cylinders, n represents the rotational speed, and g_b represents the fuel consumption rate per cycle for a single cylinder. τ represents the stroke.[40]

$$\eta_c = 1 - \frac{\Sigma x_i Q_{LHV_i}}{\left[\dot{m}_{fuel} \big/ (\dot{m}_{air} + \dot{m}_{fuel}) \right] \cdot Q_{LHV_{fuel}}} \tag{6}$$

where η_c represents the mass fraction of CO, H2, HC, and particulates. Q_{LHVi} represents the low calorific value of the corresponding component. $\dot{m}_{fuel}$ and $\dot{m}_{air}$ represent the mass flow rates of fuel and air. $Q_{LHVfuel}$ represents the low calorific value of the fuel.

Table 2. Main Equipment and Apparatus

category	measuring instruments	manufacturer	accuracy
dynamometer	CW260	CAMA	torque: ± 0.5 NM speed: ± 2 rpm
cylinder pressure sensor	6052C	Kistler	
fuel flow meter	FX-100	ONO-SOKKI	$\pm 0.12\%$
air flow meter	20R100	TOCEL	$\pm 1\%$
CO and CO_2	NDIR500	Cambustion	<2% FS/h
HC	HFR500	Cambustion	<1% FS/h
NOx	CLD500	Cambustion	<5 ppm/h
particle	DMS500	Cambustion	

$$\text{PRR} = \frac{dp}{d\varphi} \tag{7}$$

where PRR represents the pressure rise rate. $d\varphi$ represents the differential of the crankshaft angle in transverse coordinates.

The main equipment and apparatus are shown in Table 2, the physical properties of the test fuel are shown in Table 3, and the experimental conditions are shown in Table 4.

Table 3. Physicochemical Properties of Test Fuels

project	CTL	gasoline	diesel
density (15 °C)/(kg m^{-3})	757.0	690	840.0
cetane number (CN)	75.4	13	52.9
low heating value/(MJ kg^{-1})	43.07	42	42.69
total aromatics content/%	0.8	0	3.6
viscosity/(mm^2 s^{-1})	2.14	0.59	4.27
sulfur content/10^{-6}	0.38	∼	3.7
boiling point/°C	257.8	25−215	180−360
latent heat of vaporization/(MJ kg^{-1})	∼	0.29−0.315	0.27
theoretical air-fuel ratio	14.96	14.7	14.3

Table 4. Experimental Conditions

experimental conditions	SOI1	SOI2
total fuel injection (mg/cycl)	5	11.7
premix ratio (gasoline to direct injection fuel energy ratio) (%)	50	50
fuel mass ratio of pilot injection and main injection (%)	30	70
SOI1(°CA ATDC)	−36, −32, −28, −24, −20	−36
SOI2(°CA ATDC)	−10	−4, −6, −8, −10, −12
injection pressure (MPa)	100	100
intake flow rate (kg.h^{-1})	35	35
EGR rate (%)	15	15

■ AUTHOR INFORMATION

Corresponding Author

Hao Zhang − State Key Laboratory of Automotive Simulation Control, Jilin University, Changchun 130025, China; ⊙ orcid.org/0000-0002-7499-5114; Email: haozhang@jlu.edu.cn

Authors

Donghui Pan − State Key Laboratory of Automotive Simulation Control, Jilin University, Changchun 130025, China; Jilin Jianzhu University, Changchun 130118, China

Wanchen Sun − State Key Laboratory of Automotive Simulation Control, Jilin University, Changchun 130025, China

Liang Guo − State Key Laboratory of Automotive Simulation Control, Jilin University, Changchun 130025, China

Shaodian Lin − State Key Laboratory of Automotive Simulation Control, Jilin University, Changchun 130025, China

Mengqi Jiang − State Key Laboratory of Automotive Simulation Control, Jilin University, Changchun 130025, China

Complete contact information is available at:
https://pubs.acs.org/10.1021/acsomega.3c10315

Notes

The authors declare no competing financial interest.

■ REFERENCES

(1) Zhou, X.; Zhang, H.; Qiu, R.; Lv, M.; Xiang, C.; Long, Y.; Liang, Y. A Two-Stage Stochastic Programming Model for the Optimal Planning of a Coal-to-Liquids Supply Chain under Demand Uncertainty. *J. Clean. Prod.* **2019**, *228*, 10−28.

(2) Qin, S.; Zhang, X.; Wang, M.; Cui, H.; Li, Z.; Yi, W. Comparison of BGL and Lurgi Gasification for Coal to Liquid Fuels (CTL): Process Modeling, Simulation and Thermodynamic Analysis. *Energy* **2021**, *229*, 120697.

(3) Zhang, Z.; Zhang, C.; Cai, P.; Jing, Z.; Wen, J.; Li, Y.; Wang, H.; An, L.; Zhang, J. The Potential of Coal-to-Liquid as an Alternative Fuel for Diesel Engines: A Review. *J. Energy Inst.* **2023**, *109*, 101306.

(4) Shi, J.; Wang, T.; Zhao, Z.; Yang, T.; Zhang, Z. Experimental Study of Injection Parameters on the Performance of a Diesel Engine with Fischer−Tropsch Fuel Synthesized from Coal. *Energies* **2018**, *11* (12), 3280.

(5) Hao, B.; Song, C.; Lv, G.; Li, B.; Liu, X.; Wang, K.; Liu, Y. Evaluation of the Reduction in Carbonyl Emissions from a Diesel Engine Using Fischer−Tropsch Fuel Synthesized from Coal. *Fuel* **2014**, *133*, 115−122.

(6) Gill, S. S.; Tsolakis, A.; Dearn, K. D.; Rodríguez-Fernández, J. Combustion Characteristics and Emissions of Fischer−Tropsch Diesel Fuels in IC Engines. *Prog. Energy Combust. Sci.* **2011**, *37* (4), 503−523.

(7) Dec, J. E. Advanced Compression-Ignition Engines—Understanding the in-Cylinder Processes. *Proc. Combust. Inst.* **2009**, *32* (2), 2727–2742.

(8) Hardy, W. L.; Reitz, R. D. A Study of the Effects of High EGR, High Equivalence Ratio, and Mixing Time on Emissions Levels in a Heavy-Duty Diesel Engine for PCCI Combustion. *SAE Technical Paper Series; SAE International: 400 Commonwealth Drive, Warrendale, PA, United States*, 2006.

(9) Li, J.; Yang, W.; Zhou, D. Review on the Management of RCCI Engines. *Renew. Sustain. Energy Rev.* **2017**, *69*, 65–79.

(10) Cheng, X.; Chen, L.; Hong, G.; Yan, F.; Dong, S. Modeling Study of Soot Formation and Oxidation in DI Diesel Engine Using an Improved Soot Model. *Appl. Therm. Eng.* **2014**, *62* (2), 303–312.

(11) Klingbeil, A. E.; Juneja, H.; Ra, Y.; Reitz, R. D. Premixed Diesel Combustion Analysis in a Heavy-Duty Diesel Engine. *SAE Technical Paper Series; SAE International: 400 Commonwealth Drive, Warrendale, PA, United States*, 2003.

(12) Li, J.; Yang, W.; Zhou, D. Review on the Management of RCCI Engines. *Renew. Sustain. Energy Rev.* **2017**, *69*, 65–79.

(13) Liu, H.; Tang, Q.; Ran, X.; Fang, X.; Yao, M. Optical Diagnostics on the Reactivity Controlled Compression Ignition (RCCI) with Micro Direct-Injection Strategy. *Proc. Combust. Inst.* **2019**, *37* (4), 4767–4775.

(14) Tang, Q.; Liu, H.; Ran, X.; Li, M.; Yao, M. Effects of Direct-Injection Fuel Types and Proportion on Late-Injection Reactivity Controlled Compression Ignition. *Combust. Flame* **2020**, *211*, 445–455.

(15) Cui, Y.; Zheng, Z.; Wen, M.; Tang, Q.; Geng, C.; Wang, Q.; Liu, H.; Yao, M. Optical diagnostics on the effects of reverse reactivity stratification on the flame development in dual-fuel combustion. *Fuel* **2021**, *287*, 119500.

(16) Cui, Y.; Liu, H.; Wen, M.; Feng, L.; Wang, C.; Ming, Z.; Zhang, Z.; Zheng, Z.; Zhao, H.; Wang, X.; Liu, L.; Yao, M. Optical Diagnostics and Chemical Kinetic Analysis on the Dual-Fuel Combustion of Methanol and High Reactivity Fuels. *Fuel* **2022**, *312*, 122949.

(17) Sun, Y.; Sun, W.; Guo, L.; Zhang, H.; Yan, Y.; Zeng, W.; Lin, S. An Experimental Investigation of Wide Distillation Fuel Based on CTL on the Combustion Performance and Emission Characteristics from a CI Engine. *Fuel* **2022**, *310*, 122262.

(18) Zhang, H.; Sun, W.; Guo, L.; Yan, Y.; Li, J.; Lin, S.; Wang, Q.; Sun, Y. An Experimental Study of Using Coal to Liquid (CTL) and Diesel as Pilot Fuels for Gasoline Dual-Fuel Combustion. *Fuel* **2021**, *289*, 119962.

(19) Zhang, H.; Guo, L.; Yan, Y.; Sun, W.; Li, J.; Wang, Q.; Sun, Y. Experimental Investigation on the Combustion and Emissions Characteristics of an N-Butanol/CTL Dual Fuel Engine. *Fuel* **2020**, *274*, 117696.

(20) Sun, W.; Zeng, W.; Guo, L.; Zhang, H.; Yan, Y.; Lin, S.; Zhu, G.; Sun, Y. Experimental Investigation into the Effects of Pilot Fuel and Intake Condition on Combustion and Emission Characteristics of RCCI Engine. *Fuel* **2022**, *325*, 124912.

(21) Rao, L.; Kook, S.; Kim, K. S.; Kweon, C.-B. Application of Pilot Injection Strategies for Enhanced Ignition and Combustion of a Low Reactivity Fuel in a Compression-Ignition Engine. *Appl. Therm. Eng.* **2022**, *213*, 118706.

(22) Das, P.; Subbarao, P. M. V.; Subrahmanyam, J. P. Effect of Main Injection Timing for Controlling the Combustion Phasing of a Homogeneous Charge Compression Ignition Engine Using a New Dual Injection Strategy. *Energy Convers. Manage.* **2015**, *95*, 248–258.

(23) Li, X. R.; Yang, W.; Zhao, L. M.; Liu, F. S. The Influence of Pilot-Main Injection Matching on DI Diesel Engine Combustion Using an Endoscopic Visualization System. *Fuel* **2017**, *188*, 575–585.

(24) Yousefi, A.; Birouk, M.; Guo, H. An Experimental and Numerical Study of the Effect of Diesel Injection Timing on Natural Gas/Diesel Dual-Fuel Combustion at Low Load. *Fuel* **2017**, *203*, 642–657.

(25) Dave, H.; Solanki, D.; Naik, P. Effect of Pilot Fuel Quantity and Fuel Injection Pressure on Combustion, Performance and Emission

Characteristics of an Automotive Diesel Engine. *Int. J. Thermofluids* **2024**, *21*, 100570.

(26) Wei, H.; Yao, C.; Pan, W.; Han, G.; Dou, Z.; Wu, T.; Liu, M.; Wang, B.; Gao, J.; Chen, C.; Shi, J. Experimental Investigations of the Effects of Pilot Injection on Combustion and Gaseous Emission Characteristics of Diesel/Methanol Dual Fuel Engine. *Fuel* **2017**, *188*, 427–441.

(27) Hu, J.; Yao, C.; Geng, P.; Feng, J.; Liu, M.; Li, Z.; Wang, H. Effects of Pilot Injection Strategy of Diesel Fuel on Combustion Characteristics in a Premixed Methanol-Air Mixture Atmosphere in a CVCC. *Fuel* **2018**, *234*, 1132–1143.

(28) Wang, H.; Gan, H.; Theotokatos, G. Parametric Investigation of Pre-Injection on the Combustion, Knocking and Emissions Behaviour of a Large Marine Four-Stroke Dual-Fuel Engine. *Fuel* **2020**, *281*, 118744.

(29) Sathishkumar, S.; Ibrahim, M. M. Investigation on the Effect of Injection Schedule and EGR in Hydrogen Energy Share Using Common Rail Direct Injection Dual Fuel Engine. *Int. J. Hydrogen Energy* **2021**, *46* (20), 11494–11510.

(30) Dong, Y.; Kaario, O.; Hassan, G.; Ranta, O.; Larmi, M.; Johansson, B. High-Pressure Direct Injection of Methanol and Pilot Diesel: A Non-Premixed Dual-Fuel Engine Concept. *Fuel* **2020**, *277*, 117932.

(31) You, J.; Liu, Z.; Wang, Z.; Wang, D.; Xu, Y. Impact of Natural Gas Injection Strategies on Combustion and Emissions of a Dual Fuel Natural Gas Engine Ignited with Diesel at Low Loads. *Fuel* **2020**, *260*, 116414.

(32) Huang, H.; Zhu, Z.; Chen, Y.; Chen, Y.; Lv, D.; Zhu, J.; Ouyang, T. Experimental and Numerical Study of Multiple Injection Effects on Combustion and Emission Characteristics of Natural Gas-Diesel Dual-Fuel Engine. *Energy Convers. Manage.* **2019**, *183*, 84–96.

(33) Yu, H.; Chen, J.; Duan, S.; Sun, P.; Wang, W.; Tian, H. Effect of Natural Gas Injection Timing on Performance and Emission Characteristics of Marine Low Speed Two-Stroke Natural Gas/Diesel Dual-Fuel Engine at High Load Conditions. *Fuel* **2022**, *314*, 123127.

(34) Liu, H.; Li, J.; Wang, J.; Wu, C.; Liu, B.; Dong, J.; Liu, T.; Ye, Y.; Wang, H.; Yao, M. Effects of Injection Strategies on Low-speed Marine Engines Using the Dual Fuel of High-pressure Direct-injection Natural Gas and Diesel. *Energy Sci. Eng.* **2019**, *7* (5), 1994–2010.

(35) Sun, Y.; Sun, W.; Guo, L.; Yan, Y.; Zhang, H.; Li, X. Combustion and Emission Characteristics of Diesel/n-Butanol Blends with Split-Injection and Exhaust Gas Recirculation Stratification. *J. Cent. S. Univ.* **2022**, *29* (7), 2189–2200.

(36) Zheng, Z.; Xia, M.; Liu, H.; Wang, X.; Yao, M. Experimental Study on Combustion and Emissions of Dual Fuel RCCI Mode Fueled with Biodiesel/n-Butanol, Biodiesel/2,5-Dimethylfuran and Biodiesel/Ethanol. *Energy* **2018**, *148*, 824–838.

(37) Tong, L.; Wang, H.; Zheng, Z.; Reitz, R.; Yao, M. Experimental Study of RCCI Combustion and Load Extension in a Compression Ignition Engine Fueled with Gasoline and PODE. *Fuel* **2016**, *181*, 878–886.

(38) Poorghasemi, K.; Saray, R. K.; Ansari, E.; Irdmousa, B. K.; Shahbakhti, M.; Naber, J. D. Effect of Diesel Injection Strategies on Natural Gas/Diesel RCCI Combustion Characteristics in a Light Duty Diesel Engine. *Appl. Energy* **2017**, *199*, 430–446.

(39) Liu, J.; Liu, Y.; Ji, Q.; Sun, P.; Zhang, X.; Wang, X.; Ma, H. Effects of Split Injection Strategy on Combustion Stability and GHG Emissions Characteristics of Natural Gas/Diesel RCCI Engine under High Load. *Energy* **2023**, *266*, 126542.

(40) Heywood, J. *Internal Combustion Engine Fundamentals*; McGraw-Hill, 1988.